



Unsaturated hydrocarbons adsorbed on low coordinated Pd surface: A periodic DFT study

Patricia G. Belelli^{a,*}, Ricardo M. Ferullo^{a,b}, Norberto J. Castellani^a

^a Grupo de Materiales y Sistemas Catalíticos, Departamento de Física, Universidad Nacional del Sur, Av. Alem 1253, Bahía Blanca B8000CP, Argentina

^b Departamento de Química, Universidad Nacional del Sur, Av. Alem 1253, Bahía Blanca B8000CP, Argentina

ARTICLE INFO

Article history:

Received 14 September 2009

Accepted for publication 27 November 2009

Available online 21 December 2009

Keywords:

Olefin adsorption

Pd catalyst

Stepped surface

Theoretical approach

DFT

ABSTRACT

In this work, the adsorption of several unsaturated hydrocarbon molecules on a stepped Pd(4 2 2) surface was studied. Using a periodic method based on the Density Functional Theory (DFT) formalism, different adsorption geometries for ethylene, three butene isomers (*cis/trans*-2-butene and 1-butene), acetylene and 2-butyne were investigated. The results were compared with those obtained for a free defect surface as Pd(1 1 1). The 1-butene is more stable on the free defect surface than on Pd(4 2 2). On the stepped surface, the olefins adsorb tilted towards the step and increases, in almost all the cases, the magnitude of the adsorption energy. Conversely, the 3-fold site is the most stable for the alkynes adsorption on the stepped surface, as it was found on Pd(1 1 1). The analysis of the dipole moment change indicate a charge transfer from the double bond of the olefin to the metallic surface, being higher for the Pd(1 1 1) surface. In case of the alkynes, an important back-donation is produced. Except the alkynes and the 1-butene molecule, the results show the preference of ethylene and *cis/trans*-2-butene to be adsorbed on the stepped surface. These observations are related with experimental catalytic results.

© 2009 Elsevier B.V. All rights reserved.

1. Introduction

The transition metal catalysts are usually used for the hydrogenation reactions of alkenes, alkynes, aromatics, aldehydes, ketones and carboxylic acids. The hydrogenation of these unsaturated compounds is an essential process in many chemical industries, such as pharmaceuticals, food additives, flavours and fragrances, and agrochemicals [1,2]. An example of large-scale applications involves the hydrogenation of acetylene and diene impurities, which must be removed from the C2 and C4 olefin feed stocks to prevent the catalyst deactivation [3–5]. In the latter case, the best reaction pathways imply the partial hydrogenation of the carbon–carbon triple bond to yield the corresponding olefin (for C2 feed) or the half-hydrogenation of one carbon–carbon double bond (for C4 feed). In other situations, the selective hydrogenation is also desirable, like the partial hydrogenation of edible oil to obtain the corresponding *cis*-fatty acids or the selective hydrogenation of carbon–carbon double bonds in the presence of other functional groups [6–9].

In spite of the fact that catalytic hydrogenation and isomerization reactions have been extensively studied in several works [10–12,2], an intense research activity is still progressing to obtain more selective catalysts and to understand the factors which are

important in these processes, such as operating conditions, metal dispersion, carbon deposits, promoters and additives. In particular, the dispersion of the supported metal particle is a fundamental issue to evaluate in heterogeneous catalysis due to its significant influence on the catalyst performance. Many reactions on supported metal catalysts are structure-sensitive and the reason for this demanding is not yet very clear [13,14]. Besides, the size of the metallic particle is a basic parameter that determines the kind of adsorption geometry exposed to the molecules. In large particles, crystal planes of low Miller index (terraces) are developed whose atoms have a high coordination number. When the metallic particles are small, the surface regions where these planes intersect are ever more important. The atoms pertaining to these edges have low coordination number and can be associated with defects such as steps, edge and corners. These atoms have different electronic properties than those of terraces. As a consequence the nature of the link formed between the surface Pd atoms and adsorbates with π -bonds like unsaturated hydrocarbons would be affected.

The theoretical study of the adsorption and decomposition of unsaturated hydrocarbons with different chain lengths, cycloalkenes or hydrocarbons with functional groups as aldehydes or alcohols on well-defined surfaces is an important issue to understand the surface mechanisms in catalytic reactions [15–24]. Traditionally, these studies are focused on low-index surfaces. However, catalytic surfaces of technological relevance are non-ideal and

* Corresponding author. Tel.: +54 291 4595141; fax: +54 291 4595142.

E-mail address: pbelelli@plapiqui.edu.ar (P.G. Belelli).

other studies must be performed to improve our knowledge of real catalysts. In this sense, our interest is to study the role played by surface defects in catalytic reactions. First-principle periodic calculations of surface defects are scarce and, due to the very low symmetry, limited to situations with a small number of atoms.

In the present paper the adsorption energies, binding site preferences and geometries of different unsaturated hydrocarbons on a stepped Pd surface are evaluated by means of DFT calculations. The main purpose is to compare the adsorptive properties with respect to a close packed Pd(1 1 1) surface. Palladium-based catalysts are the most used ones in industry for gas- and liquid-phase hydrogenation of alkynes and dienes [25]. This metal presents appreciably activity and chemoselectivity.

2. Surface model and computational details

All calculations reported in this work were carried out in the framework of DFT using the Vienna Ab initio Simulation Package (VASP) [26–28]. Plane wave basis sets were used to solve the Kohn–Sham equations. The electron–ion interactions are described by the projector-augmented wave method (PAW). The PAW method is a frozen core all-electron method that uses the exact shape of the valence wave functions instead of pseudo-wave functions [29,30].

The fixed convergence of the plane-wave expansion was obtained with a cut-off energy of 400 eV. Our previous tests showed that using this value the converged calculation error was lower than 0.001 eV. Electron exchange and correlation effects were described by the generalized gradient approximation (GGA), using the functional described by Perdew–Wang (PW91) [31,32]. The two dimensional Brillouin integrations were performed on a grid of $3 \times 6 \times 1$ Monkhorst–Pack special k -points for a 5×3 supercell, and of $3 \times 3 \times 1$ k -points, for a 3×3 supercell [33]. In both cases, a Methfessel–Paxton smearing of width $\sigma = 0.2$ eV was used [34]. Optimized geometries were found when the forces on atoms were smaller than 0.02 eV/Å².

The stepped Pd surface was represented with a slab containing four atomic metal layers. The effect of the slab thickness was tested considering slabs containing up to six atomic layers. The results showed that a slab with four layers provides converged results, with an accuracy higher than 0.04 eV. Therefore, a slab with four atomic layers should be appropriate to the present study. Our stepped surface consists of (1 1 1) terraces of three atoms width separated by monoatomic steps oriented parallel to the (1 0 0) face. A three dimensional periodic cell was constructed including a vacuum gap of ~ 16 Å in the perpendicular direction to the metallic surface. The thickness of this vacuum region was found to be adequate to eliminate any interaction between adjacent metal slabs.

In order to minimize the interaction between adsorbates and neighboring steps surface, a 5×3 super cell with 54 atoms distributed over four layers was used (Fig. 1). The effect of the size of the cell was tested by comparing the results corresponding to 1-butene adsorbed also on 6×3 and 5×4 super cells. They do not show significant variations in adsorption energies neither in geometrical parameters. The discrepancy observed on the adsorption energies was lower than 0.3 kcal/mol and on the optimized distances was lower than 0.01 Å among the three super cells. For this reason, the 5×3 unit cell gives energies and geometrical parameters well converged for the hydrocarbon adsorptions studied in our work. This unit cell is associated with a molecular coverage of 1/15 ML.

Regarding the effect of step width, we point out that in a previous theoretical work performed by Raouafi et al. [35] the variation of the step energy as a function of the terrace width for different stepped surfaces was studied. In case of Pd metal, the step energies

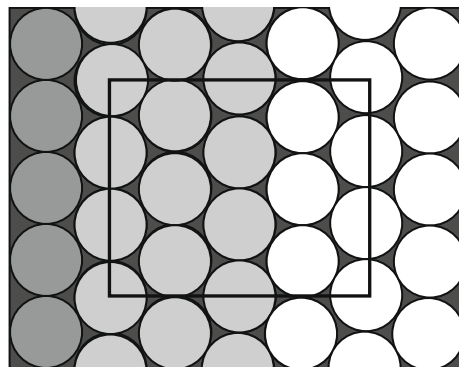


Fig. 1. 5×3 Supercell used to represent the stepped Pd surface.

for the stepped surface $p(1\ 1\ 1) \times (1\ 0\ 0)$ (where p means the number of rows at the terrace) varies only by nearly 0.004 eV (per step atom) from $p = 3$ to $p = 7$. In our surface model, $p = 3$. According to the Somorjai notation [36], the Miller indices for the stepped surface $p(1\ 1\ 1) \times (1\ 0\ 0)$ are $(p + 1, p - 1, p - 1)$, where $p + 1$ also denotes the number of rows at the terraces that are parallel to the steps. In our ideal stepped surface with $p = 3$, the Miller indices are (4, 2, 2).

The interaction between the adsorbate states and the metal d states is the main physical factor that defines the chemisorption energy. The d -bands are narrow and small changes in the environment can modify significantly the d states and their interaction with adsorbate states [37]. As a general rule it can be stated that the lower the coordination number, the smaller the local bandwidth and the higher the d -band center [38]. According to this rule, the d -band centers calculated from the local density of states (LDOS) for edge Pd atoms in Pd(4 2 2) and regular surface atoms in Pd(1 1 1) are at -1.88 eV Pd(4 2 2) and -1.97 eV, respectively.

Different unsaturated hydrocarbons were adsorbed on the stepped Pd surface. The adsorbate species were placed in one side of the slab and their geometries were allowed to optimize completely together with the two uppermost layers of the surface. The remaining atoms of the slab were frozen at the bulk optimized positions (with a Pd–Pd interatomic distance of 2.80 Å). The adsorption energy (E_{ads}) was calculated as the difference between the energy of the adsorbed molecule ($E_{\text{adsorbate/surface}}$) and the sum of the free surface (E_{surface}) and the gas-phase molecule ($E_{\text{gas-phase}}$) energies. A negative value indicates an exothermic chemisorption process. A large box of $20 \times 15 \times 15$ Å³ was used to obtain the gas-phase molecule energies. The optimized geometries of the free unsaturated hydrocarbons predict bond distances and bond angles in agreement with previous experimental and theoretical results [15,18,39].

The electronic structure of the adsorbate/Pd interaction was analyzed by calculating the Local Density of States (LDOS) at selected atoms and the change of the work function ($\Delta\Phi$). $\Delta\Phi$ was obtained as the difference between the work function of the surface with and without adsorbed molecules. The work function itself was obtained by computing the electrostatic potential of the corresponding surface. The dipole moment (μ) was also evaluated by integration over the entire cell. The dipole moments were calculated by numerical integration of charge densities obtained from single point energy calculations on relaxed structures, as implemented in VASP. This vector is considered as positive going from the positive charge towards the negative charge. The dipole moments were obtained considering different contributions [40].

3. Results and discussion

3.1. Adsorption of alkenes

First, the di- σ and π adsorption modes of ethylene, *cis/trans*-2-butene and 1-butene on a stepped Pd surface were evaluated. In Table 1 the adsorption energies and the main geometrical parameters are summarized while in Fig. 2 the optimized geometries of these molecules in di- σ and π adsorption modes on the stepped Pd surface are presented.

Regarding the adsorption energies of the alkenes, we observe that generally the di- σ adsorption mode is slightly preferred with respect to the π mode, with a relatively small difference between their adsorption energies. Only the *trans*-2-butene adsorbed on π site of this stepped surface has the E_{ads} greater than on the di- σ site. In this case, the optimized geometrical configuration presents the C=C double bond not aligned with the edge of the step (see Fig. 2f). The butene isomers adsorbed on their most preferred sites have the following stability: *trans*-2-butene > *cis*-2-butene \gg 1-butene; the latter isomer being the lowest stable on both adsorption sites. The adsorption of ethylene is stronger on the di- σ site than π site as it was observed with other coverages and surfaces [15,17,20,41,42]. Ethylene adsorbed on the di- σ site is more stable than 2-butenes isomers. In fact, the increase of the chain length produces a slight destabilization of the olefins as one goes from ethylene to *cis/trans*-2-butene isomers, with an even greater decrease for 1-butene. On the other hand, Neurock et al. [24] found that the greater decreases was obtained from ethylene to 1-propylene, remaining afterwards with a similar value for higher olefins if they are adsorbed on terrace surfaces of bimetallic catalysts composed with Pt. This trend was not observed for the olefins evaluated in this work, likely due to the better geometrical rearrangement of olefins when are adsorbed on a defective surface.

As a general rule, the interaction of the olefin with the metallic surface is mainly through the C=C double bond, accompanied by a bending of the hydrogen or alkyl groups away from the surface. In all the cases, the original planarity of the free molecules is broken, which is an evidence of some degree of rehybridization of the carbon atomic orbitals. Regarding the internal geometry of adsorbed alkenes, the C=C double bond is significantly longer than in the free molecule; for all the adsorbates, the lengthening is of nearly 0.1 Å. The interaction with the metal surface in the di- σ sites takes place at shorter Pd–C interatomic distances than when the adsorp-

tion is in π sites, for example at 2.14 and 2.15 Å for ethylene and 1-butene in di- σ sites and at 2.21 and 2.23 Å for ethylene and 1-butene in π sites, respectively. This behavior is also observed for *cis/trans*-2-butene. The equilibrium geometries of the adsorbed molecules are tilted with respect to the terrace plane, in a way to decrease the steric hindrance of the alkyl groups with the metal surface. The α angle, which is formed by the C–Pd bond and the normal to the Pd(1 1 1) terrace of the step, measures this inclination (see Table 1). The di- σ adsorption mode presents larger α angles than the π mode, i.e., the molecules in the first case are ~ 30 – 40° more tilted than in the second case.

It is well-known that the work function is highly dependent on the distribution of charges in the molecule/substrate system. Particularly, its change $\Delta\Phi$ with respect the bare metal surface is directly associated with the value of the dipole moment change $\Delta\mu$ induced by the molecule on the surface. In Table 1 the values of $\Delta\Phi$ and $\Delta\mu$ for different olefins are summarized. The negative values of $\Delta\Phi$ indicate that the presence of adsorbates become easier the extraction of an electron from the surface. In general, the magnitude of $\Delta\Phi$ is lower on di- σ than on π sites, with the exception of *trans*-2-butene where the same magnitude of $\Delta\Phi$ for both sites were obtained.

In order to understand these results, the $\Delta\mu$ generated by the molecules adsorbed on stepped surface were evaluated. In the situation where the effects from Pauli repulsion can be discarded, $\Delta\mu$ is associated with two main contributions: that due to the individual molecules ($\mu_{\text{adsorbate}}$) and that due to the charge reordering upon chemisorption (μ_{transf}) [40]. The molecules studied in this work do not present intrinsic dipole moments in gas phase. However, when they adsorb on the Pd surface, non-negligible dipole moments appear because their initial geometries are modified and the electronic charge becomes distorted. For this reason, the $\mu_{\text{adsorbate}}$ must be calculated considering the adsorption geometry of the molecules, but without the presence of the metal surface. In our adsorbate/substrate systems, the coverage is fixed and then any effect due to molecule–molecule interactions is included in the $\mu_{\text{adsorbate}}$ calculation. In particular, the values of $\mu_{\text{adsorbate}}$ on di- σ sites are higher than on π sites due to the greater deformation in contact with the surface, in agreement with our previous analysis of their equilibrium geometries.

The dipole moments due to the charge transfer, μ_{transf} , were obtained after subtracting of $\mu_{\text{adsorbate}}$ from $\Delta\mu$. Looking at Table 1, a first observation is that the adsorption of olefins always produces

Table 1
Adsorption energies (E_{ads} in kcal/mol), work function change ($\Delta\Phi$ in eV), dipole moments (μ in Debye) and relevant geometric parameters of olefins adsorbed on stepped surface Pd(4 2 2).^a

Adsorbate	Ethylene		<i>Cis</i> -2-butene		<i>Trans</i> -2-butene		1-Butene	
	di- σ	π	di- σ	π	di- σ	π	di- σ	π
E_{ads}	–28.2	–26.0	–25.7	–24.9	–26.0	–27.3	–19.9	–17.9
$\Delta\Phi$	–0.46	–0.54	–0.84	–1.03	–0.84	–0.83	–0.75	–0.85
$\Delta\mu$	–1.55	–2.03	–3.15	–3.68	–3.01	–3.12	–2.92	–3.25
$\mu_{\text{adsorbate}}$	–0.49	–0.44	–0.80	–0.71	–0.71	–0.61	–0.86	–0.64
μ_{transf}	–1.06	–1.59	–2.35	–2.97	–2.30	–2.51	–2.06	–2.61
d(Pd–C)	2.14	2.21	2.16	2.25	2.17	2.24	2.15	2.23
d(C=C)	1.43	1.39	1.43	1.40	1.43	1.40	1.43	1.39
d(C–C)	–	–	1.51	1.51	1.52	1.50	1.52	1.51
$\langle\text{C–C=C}\rangle^b$	117.7	120.4	120.6	125.2	120.7	124.0	120.1	123.9
$\langle\text{Pd–C=C}\rangle$	108.0	71.7	107.6	71.9	106.7	72.1	108.2	71.5
$\langle\text{Pd–Pd–C}\rangle$	72.0	74.3	72.4	75.4	72.2	77.9	72.0	74.9
α^c	54.9	12.0	55.7	19.0	46.6	76.2 9.5 27.4	43.2	16.3

^a Distances expressed in Armstrong (Å) and bond angles in degrees ($^\circ$).

^b In case of ethylene molecule the angle corresponds to H–C=C.

^c α Angle is formed by C–Pd bond and the surface normal.

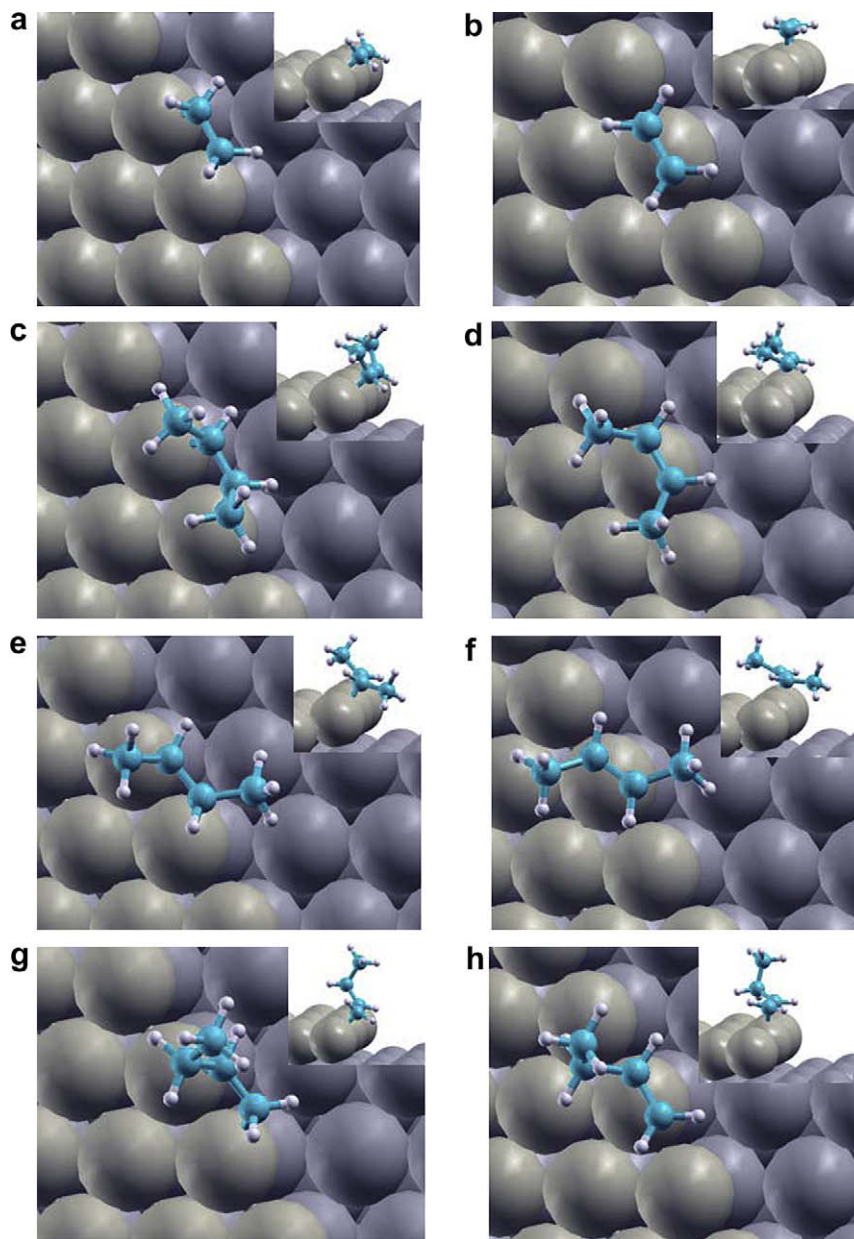


Fig. 2. Optimized adsorption geometries for adsorbed alkenes on the stepped Pd(4 2 2) surface. Di- σ and π adsorption modes for: (a–b) ethylene, (c–d) *cis*-2-butene, (e–f) *trans*-2-butene and (g–h) 1-butene, respectively. Two different grey colours were used to clarify the step edge.

negative μ_{transf} values. These negative values show the dominant effect of electronic charge donation from the molecules to the metallic surface rather than the back-donation to the molecules. Comparing both adsorption sites, we observe that the olefins generally release a greater electronic charge on π sites than on di- σ sites, i.e., μ_{transf} is enhanced from $\sim 30\%$ to 50% on these sites. In other words, the unbalance of donation/back-donation is more notorious for π sites, where the magnitude of the adsorption energy is smaller. Therefore, the weaker bonding on π sites can be attributed to a less relevant back-donation effect. The exception is *trans*-2-butene, where the π site is more favoured. However, in this case the μ_{transf} is increased only in 9% with respect to the di- σ site. The μ_{transf} for ethylene is lower than the values observed for butenes isomers. This behavior can be related with the electron-donating effect of the methyl groups in butane molecules with respect to ethylene. Analyzing the magnitude of $\mu_{\text{adsorbate}}$ and μ_{transf} contributions to $\Delta\mu$, it is possible to observe that the lat-

ter are bigger, being from twice to four times higher than $\mu_{\text{adsorbate}}$. For this reason, the work function change is mainly due to the charge transfer between adsorbate and the metallic surface.

The electronic structure that governs the chemical bonding between molecule and substrate has been analyzed through the LDOS, which were calculated on interacting Pd and C atoms. In particular we are interested in the change in the d -band of Pd atoms after the olefin adsorption, with respect to the bare surface. For both di- σ and π adsorption modes, the C=C double bond is generally in the same direction of the Pd atoms at the edge of the step. This geometry favours the overlapping between the d -orbitals of Pd atoms and the p -orbitals of C atoms producing a significant splitting of the d -band. Furthermore, the center of the occupied d -band shows a displacement to lower energies in comparison with the free metallic surface. These observations can be rationalized taking into account that the states at the bottom of the d -band are more involved in the interaction with HOMO and HOMO-1

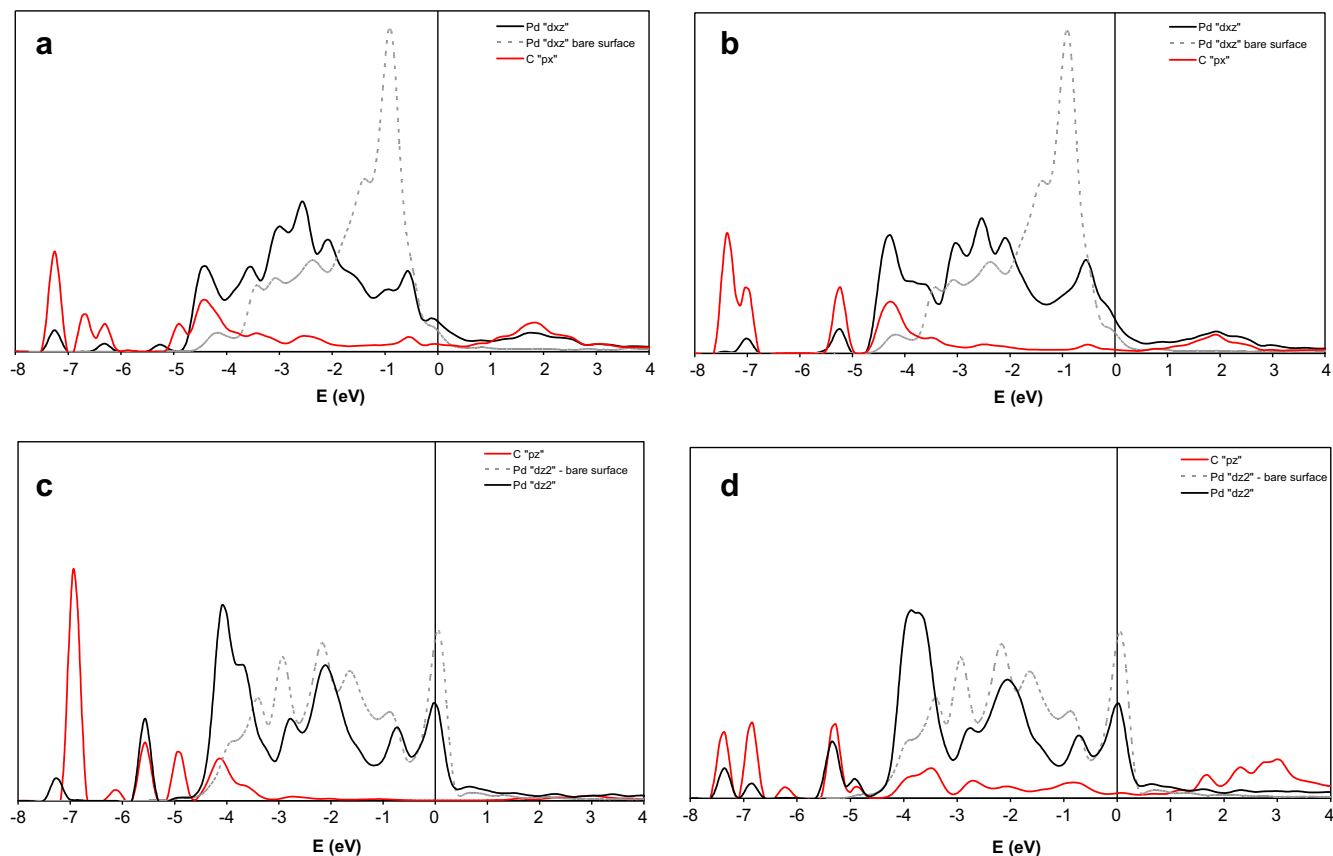


Fig. 3. LDOS for *cis*-2-butene and *trans*-2-butene molecules adsorbed on the stepped Pd surface. On di- σ site: (a) *cis*-2-butene and (b) *trans*-2-butene. On π site: (c) *cis*-2-butene and (d) *trans*-2-butene.

orbitals of the olefin. On the other hand, the states at the top of the d -band are mainly involved in the interaction with the LUMO orbital of the adsorbate generating the displacement of states above the Fermi level. For further analysis, we point out that for *cis/trans*-2-butene isomers in gas phase only the Cp_z atomic orbital participates in the HOMO and LUMO molecular orbitals, while in the HOMO-1 exclusively contributes the Cp_x atomic orbital.

For the di- σ adsorption mode, the main interaction occurs between the d_{xz} and p_x orbitals of Pd and C atoms, respectively. In case of the *cis/trans*-2-butene isomers, the center of the occupied d_{xz} band shows a binding energy shift of -1.0 eV with respect to the clean surface where the band center is at ~ -1.7 eV (see Fig. 3a and b). In case of *cis*-2-butene/Pd(4 2 2) system, the presence of a peak at ~ -7.2 eV and a feature at -4.5 eV would correspond respectively to the bonding and antibonding combinations between the adsorbate HOMO-1 orbital (where the Cp_x atomic orbital mainly participates) and the d_{xz} band of Pd. On the other hand, the flat band at 2 eV results from the combination between the higher unoccupied π^* orbital of *cis*-2-butene and the d_{xz} band of Pd. A similar analysis can be performed for the *trans*-2-butene/Pd(4 2 2) system. Besides, a non-negligible mixing of Cp_x and d_z^2 band is also produced. For *cis*-2-butene, a band at about -5 eV and a double peak at -6.3 and -6.7 eV were observed at the LDOS of Cp_x and d_z^2 band (not shown), while for *trans*-2-butene we have a band at about -5.2 eV and a double peak at -7.0 and -7.4 eV. On the other hand, a coupling between the d_z^2 and p_z orbitals of Pd and C atoms respectively also takes place, but it is of smaller importance than that of previous mentioned orbitals. The displacement of d_z^2 band center is of ~ -0.5 eV downward with respect to the clean stepped surface ($\langle E_{dz}^2 \rangle$ at -2.1 eV). It is worth emphasizing

that when the molecule resides on the regular Pd(1 1 1) surface, the interacting orbitals are mainly Pd d_z^2 and Cp_z [21].

When the olefin adsorbs in the π mode, the coupling between the palladium d_z^2 and carbon p_z orbitals is more relevant than the coupling between the palladium d_{xz} and carbon p_x orbitals. In case of the *cis/trans*-2-butene isomers, the displacement of the center of the occupied d_z^2 band is of -0.8 eV downward with respect to the clean stepped surface (Fig. 3c and d). For the *cis*-2-butene/Pd(4 2 2) system, the presence of a peak at ~ -5.6 eV and a feature at -4.1 eV would correspond to the bonding and antibonding combinations between the adsorbate HOMO orbital (where the Cp_z atomic orbital mainly participates) and the d_z^2 band of Pd. A similar analysis is valid for the *trans*-2-butene/Pd(4 2 2) system. However, no relevant mixing can be observed between the LUMO of *cis*-2-butene and the d_z^2 band of Pd. This result is compatible with the fact that for this site the electronic back-donation to the LUMO of *cis*-2-butene is much less important than the donation from the HOMO, as it was commented above using μ_{transf} arguments. Furthermore, a non-negligible mixing of Cp_z and d_{xz} band is also produced. For *cis*-2-butene, the peaks at about -6.9 eV and at -5.0 eV were observed at the LDOS of Cp_z and Pd d_{xz} (not shown), while for *trans*-2-butene these same contributions were at -7.4 eV and -6.8 eV.

In order to evaluate the effect of surface morphology on olefins adsorption, the chemical bonding of these molecules with a perfect Pd(1 1 1) surface was also studied by using the same theoretical approach on a 3×3 supercell (associated with a molecular coverage of 1/9 ML). The corresponding adsorption energies and geometrical parameters are summarized in Table 2. For the olefins here studied, the di- σ adsorption mode is slightly preferred with respect to the π mode. In the particular case of ethylene, the di- σ mode is slightly more stable by ~ 3 kcal/mol than previous

Table 2

Adsorption energies (E_{ads} in kcal/mol), work function change ($\Delta\Phi$ in eV), dipole moments (μ in Debye) and relevant geometric parameters of olefins adsorbed on surface Pd(1 1 1).^a

Adsorbate	Ethylene		Cis-2-butene		Trans-2-butene		1-Butene	
	di- σ	π	di- σ	π	di- σ	π	di- σ	π
E_{ads}	-23.9	-20.4	-19.5	-17.6	-19.5	-17.3	-20.6	-17.9
$\Delta\Phi$	-1.03	-1.20	-1.63	-1.85	-1.64	-1.92	-1.60	-1.68
$\Delta\mu$	-2.07	-2.38	-3.50	-3.94	-3.45	-4.05	-3.19	-3.53
$\mu_{\text{adsorbate}}$	-0.85	-0.49	-1.09	-0.76	-1.22	-0.83	-1.06	-0.68
μ_{transf}	-1.22	-1.89	-2.39	-3.18	-2.23	-3.22	-2.13	-2.85
d(Pd-C)	2.13	2.19	2.15	2.24	2.14	2.23	2.14	2.20
								2.24
d(C=C)	1.45	1.40	1.46	1.41	1.47	1.41	1.45	1.40
d(C-C)	-	-	1.51	1.50	1.52	1.51	1.52	1.51
$\langle\text{C-C=C}\rangle^{\text{b}}$	116.8	120.3	119.8	123.6	117.4	122.3	119.3	123.1
$\langle\text{Pd-C=C}\rangle$	107.8	71.4	107.2	71.7	107.3	71.6	107.6	70.2
$\langle\text{Pd-Pd-C}\rangle$	72.2	75.9	72.8	78.0	72.7	78.4	74.9	74.1

^a Distances expressed in Armstrong (Å) and bond angles in degrees (°).

^b In case of ethylene molecule the angle corresponds to H-C=C.

reported results [17], due to the lower coverage used in this work ($\theta = 0.11$ ML vs. $\theta = 0.25$ ML, respectively). Our results indicate that the different butene isomers adsorbed on di- σ site have the following stability: 1-butene > *trans*-2-butene \cong *cis*-2-butene. On the other hand, the three isomers have almost the same stability for the π site. These results as well as the geometric ones show the same trends as those obtained by other authors [39]. Ethylene is more stable than the butene isomers for both types of sites.

The adsorption energy values for the regular surface are generally lower in magnitude than those for the stepped surface by nearly 7–10 kcal/mol, with the exception of 1-butene, where it is slightly greater for the di- σ site or equal for the π site. The $\Delta\Phi$ values for the (1 1 1) surface (see Table 2) are negative as those for the (4 2 2) surface, suggesting an electronic transfer from the adsorbed molecules to the metal. For Pd(1 1 1), the magnitude of $\Delta\Phi$ is about 50% higher due mainly to the larger coverage (1/9 vs. 1/15 ML). On the other hand, the $\Delta\mu$ value, which is a physical property normalized per adsorbed molecule, is at least 0.3 Debye greater for the (1 1 1) surface. As it was commented for the stepped surface, the values of $\mu_{\text{adsorbate}}$ on di- σ sites are higher than on π sites due to the greater deformation in contact with the surface. This deformation is even more pronounced on (1 1 1) surface than on stepped surface. Once more, the sign of the μ_{transf} contribution to $\Delta\mu$ indicates that an electronic transfer is produced from the molecule to the metal rather than a back-donation to the molecules. Its magnitude is in general larger than on the stepped surface, indicating that the adsorptions are governed by stronger donation effects of the molecules than back-donation effects.

Studies accomplished by Freund et al. [43,44] have shown that the catalytic hydrogenation of 1,3-butadiene on Pd catalyst is a *structure-sensitive* reaction, i.e., Pd(1 1 0) is 5-fold more active than Pd(1 1 1). Subsequent studies of the same authors pointed out that this reaction is *particle size independent* if the number of Pd atoms in the (1 1 1) facets is used to normalize the number of converted 1,3-butadiene molecules [45,46]. The Pd nanoparticles with sizes larger or equal to 4 nm, considering that they have a truncated cubo-octahedral shape with (1 1 1) and (1 0 0) surface facets, present similar activity to Pd(1 1 1) single crystal. In the initial state of reaction, the hydrogenation of 1,3-butadiene produces 1-butene, *trans*-2-butene and *cis*-2-butene as primary products, independently of the Pd particle size in the catalyst [46]. After complete consumption of diene, the 1-butene molecule readsorbs yielding *n*-butane by hydrogenation and *cis/trans*-2-butene through isomerization. The experiments show that on the Pd(1 1 1) single crystal, the *n*-butane was produced before the diene was completely consumed; thus, the selectivity of Pd nanoparticles toward butenes

turns out to be higher than that of Pd(1 1 1), giving lower amount of *n*-butane. In relation to this point, our theoretical results indicate that the higher binding energy for 1-butene on Pd(1 1 1) could be a reason why this isomer is primarily readsorbed and hydrogenated. The situation is different in the case of the (4 2 2) surface. Here, the magnitude of E_{ads} changes in the following order: *trans*-2-butene \cong *cis*-2-butene \gg 1-butene, with an energy difference of 27% for 1-butene with respect to *trans*-2-butene. If we assume that the catalytic particles have a greater amount of line defects, it would be expected that the 1-butene yield would not decrease significantly. Nevertheless, the 1-butene readsorbs producing more *cis/trans*-2-butene and *n*-butane [45]. From the experimental and our theoretical data previously commented, we can infer that the hydrogenation of 1-butene occurs preferentially on the Pd(1 1 1) facets of Pd particles than on line defects of these particles. Taking into account that the line defects could be represented by our stepped Pd model, they would be occupied by the *cis/trans*-2-butenes, while the 1-butene would adsorb on the (1 1 1) facet of the Pd nanoparticles. This is a consequence of the slightly better stability of 1-butene on this surface (energy difference of ~ 0.8 kcal/mol) with respect to the stepped surface. Regarding the improved selectivity for isomerization on nanoparticles, it may be due to the poor hydrogen accessibility to the metallic surface, because the Pd(1 1 1) facet would be occupied by 1-butene and the line defects of the particles by *cis/trans*-2-butene. In this situation, the 1-butene hydrogenation would be disfavoured and the isomerization would take place. Experimental evidences indicate that, after 1,3-butadiene hydrogenation, the surface structure do not undergo relevant changes [46]. Furthermore, the presence of a small amount of carbon deposit do not affect the reaction performed up to 500 K [44]; neither, no Pd-C phase was observed for 1-pentene, propene and ethylene hydrogenation at ~ 350 K on Pd foil catalyst [47].

3.2. Adsorption of alkynes

The adsorption of acetylene and 2-butyne on di- σ and π sites of the stepped Pd(4 2 2) surface were investigated. Besides, an additional adsorption site was also evaluated. Taking into account different experimental works indicating that the acetylene molecule binds on the 3-fold hollow sites of Pd(1 1 1) [48–50], this type of site was also considered. In Table 3 the adsorption energies and the main geometrical parameters for these three adsorption modes on this surface are summarized. In Fig. 4a–c and d–f the corresponding equilibrium geometries for acetylene and 2-butyne on di- σ , π and 3-fold hollow adsorption modes are exhibited,

Table 3

Adsorption energies (E_{ads} in kcal/mol), work function change ($\Delta\Phi$ in eV), dipole moments (μ in Debye) and relevant geometric parameters of alkynes adsorbed on stepped surface Pd(4 2 2).^a

Adsorbate Adsorption mode	Acetylene			2-Butyne		
	di- σ	π	3-Fold	di- σ	π	3-Fold
E_{ads}	-31.0	-24.8	-41.6	-23.4	-15.7	-24.4
$\Delta\Phi$	-0.27	-0.55	-0.56	-0.78	-1.17	-0.89
$\Delta\mu$	-0.97	-1.98	-1.62	-2.93	-4.35	-3.38
$\mu_{\text{adsorbate}}$	-1.53	-0.87	-1.55	-1.99	-1.25	-2.11
μ_{transf}	0.56	-1.11	-0.07	-0.94	-3.10	-1.27
d(Pd-C)	2.00	2.13	2.00	2.01	2.17	2.03
d(C \equiv C)			2.18			2.25
d(C-C)	1.31	1.26	1.36	1.32	1.25	1.36
(C-C \equiv C) ^b	-	-	-	1.50	1.47	1.50
(Pd-C \equiv C)	131.9	155.3	128.2	132.2	156.0	128.8
(Pd-Pd-C)	112.9	72.9	71.8	111.6	73.3	72.4
			113.1			112.4
	67.1	75.3	66.8	68.5	77.9	67.6
α^c	1.6	13.3	55.8	7.1	4.2	64.3

^a Distances expressed in Armstrong (\AA) and bond angles in degrees ($^\circ$).

^b In case of acetylene molecule the angle corresponds to H-C \equiv C.

^c α Angle is formed by C-Pd bond and the surface normal.

respectively. On this stepped surface, the 3-fold hollow site has two Pd atoms located on the edge of the step.

For acetylene and 2-butyne, the di- σ adsorption mode is preferred with respect to the π mode, as it was also observed for olefins, but with a more significant energy difference (by near 7 kcal/mol). For both alkynes, the better stability was obtained on the 3-fold hollow site; the energy difference with respect to the di- σ site is of nearly 10 kcal/mol for acetylene and only of 1 kcal/mol for 2-butyne.

Regarding the adsorption geometries of alkynes, we notice that the chemical links with the Pd surface for the di- σ and π adsorption modes are through the C \equiv C bond, with the Pd-C bonds shorter than in olefin adsorption. However, the acetylene and 2-butyne molecules adsorb for both di- σ and π modes on the edge of the

step with only a very small tilting ($\alpha \leq 13^\circ$). The interatomic distance of the C \equiv C bond is up to 0.1 \AA longer than in the free molecule, while the H-C \equiv C and C-C \equiv C angles change significantly from 180 $^\circ$ in gas phase to 132 $^\circ$ and 156 $^\circ$ for di- σ and π sites, respectively. In the 3-fold hollow mode, the C atoms change the hybridization from a sp to a sp² configuration due to the double interaction of each C atom with the Pd surface. After the adsorption, the interatomic C-C distance increases by 0.15 \AA , while the H-C \equiv C and C-C \equiv C angles decreases by 52 $^\circ$.

In Table 3 the values corresponding to $\Delta\Phi$, $\Delta\mu$ and the two contributions $\mu_{\text{adsorbate}}$ and μ_{transf} for the alkynes are summarized. The negative value of $\Delta\Phi$ indicates like for the olefins that the presence of adsorbate molecules become easier the extraction of an electron from the surface. For both alkynes, the values of $\Delta\Phi$ are more negative on π than on di- σ sites. On the other hand, the magnitude of $\mu_{\text{adsorbate}}$ is greater than for the olefins, due to the larger deformations undertaken by the alkynes; in addition and for the same reason they are higher on di- σ sites than on π sites. The values of μ_{transf} corresponding to acetylene on di- σ and π sites are more positive than for ethylene adsorbed in the same sites. This observation can be explained taking into account the large electronegativity of acetylene that produces an important back-donation from the *d*-orbitals of the metal to the empty π^* antibonding orbitals of acetylene. Consequently, we have a stronger bonding to the metal than that obtained for the correspondent olefin (ethylene). For acetylene on the di- σ site, μ_{transf} has a positive value and the charge transfer goes from the Pd surface to the adsorbate. In case of 3-fold site, the value of μ_{transf} is very small indicating that no charge transfer occurs; for this reason, $\Delta\Phi$ is exclusively due to the dipole moment of the acetylene layer. In case that the C \equiv C triple bond has methyl substituents like in 2-butyne the donation increases, i.e., more negative values of μ_{transf} are obtained in the three adsorption sites and the molecule-metal bond becomes less strong (Table 3). Comparing the alkynes on the same adsorption site, it is possible to observe that the $\Delta\Phi$ values are less negative when the back-donation is increased.

The local density of states (LDOS) calculated on Pd and C atoms for the alkyne/Pd(4 2 2) systems reveal some common features just

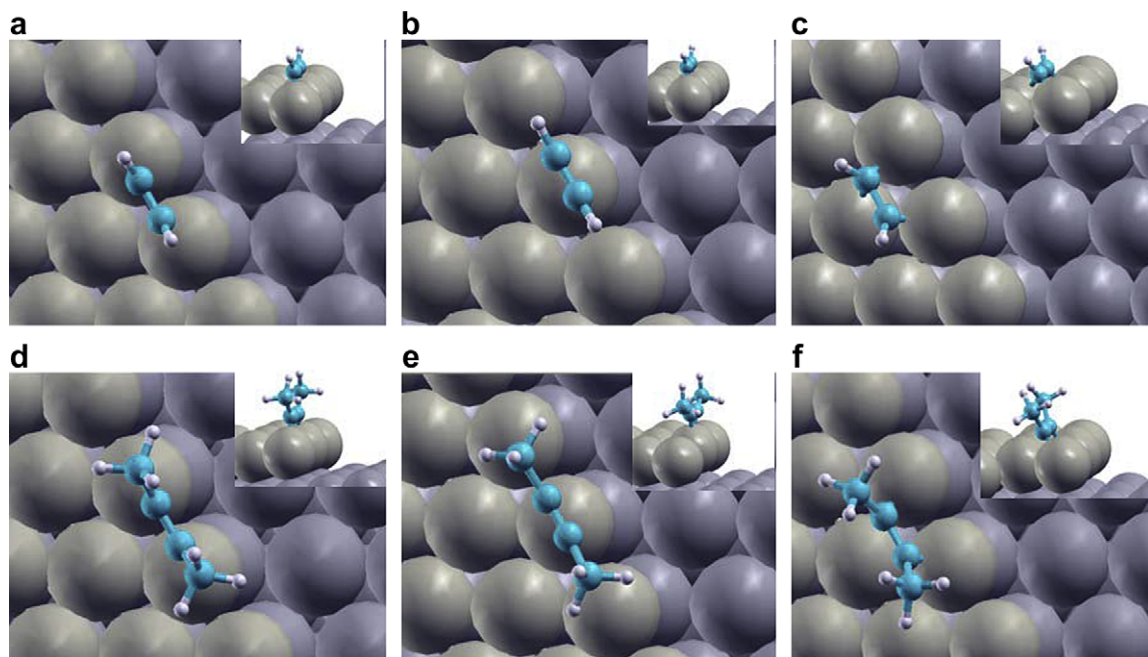


Fig. 4. Optimized adsorption geometries for adsorbed alkynes on the stepped Pd(4 2 2) surface. Di- σ , π and 3-fold hollow adsorption modes for: (a-c) acetylene and (d-f) 2-butyne, respectively. Two different grey colours were used to clarify the step edge.

outlined for the olefin adsorptions. As for alkenes adsorbed on di- σ and π sites, the $C\equiv C$ triple bond is placed parallel above the edge of the step where the interacting Pd atoms are, favouring the overlapping between the Pd d -band and Cp atomic orbitals. Then, a significant splitting of the d -band is produced, together with a downward displacement of its center (for the occupied states) in comparison with the bare metallic surface. This observation is particularly notorious for the di- σ adsorption mode, because in this situation the alkynes molecules are not tilted as was the case of alkenes, producing an important overlap between the $Pd d_z^2$ and Cp_z atomic orbitals (Fig. 5a and b). For the acetylene molecule adsorbed on the di- σ site, the center of the occupied d_z^2 band shifts downward by about -1.3 eV with respect to the clean surface ($E_{d_z^2}^0$ at -2.1 eV). At least part of this behavior can be due to the fact that the Pd surface releases a significant amount of electron charge through the back-bonding mechanism to acetylene (as it was previously mentioned in the analysis of μ_{transf}). The presence of two peaks at ~ -7.4 eV and -5.1 eV would correspond respectively to the bonding and antibonding combinations between the adsorbate HOMO orbital and the d_z^2 band. On the other hand, the flat band at -4.0 eV, with a feature at energies higher than the Fermi level could be due to the combination between the higher unoccupied π^* orbital of acetylene and the d_z^2 band of Pd. For the 2-butyne molecules adsorbed on the di- σ site, we have also two peaks at -7.4 eV and at -6.8 eV which would correspond to the bonding and antibonding combinations between HOMO and d_z^2 band.

When the alkyne adsorbs on the 3-fold site, the d_z^2 band and the Cp_z orbital couple, but less strongly than on the di- σ site. On this site, the d_{yz} band and the Cp_y orbitals play the main role in the interactions (see Fig. 5c and d). For acetylene, the peaks at -8.0 eV and at -5.8 eV would correspond to the bonding and anti-

bonding combinations of acetylene HOMO and d_{yz} band. The presence of these peaks at higher binding energies than on the di- σ site is in agreement to the relatively large electronic back-bonding from the surface Pd atoms for the last type of site (as it was previously analyzed with μ_{transf}).

For the sake of comparison, the chemical bonding of these alkynes was also studied on a perfect Pd(111). The corresponding adsorption energies and geometrical parameters are summarized in Table 4. In agreement with other DFT studies [18], we find for acetylene that the preference site decreases in the following order: 3-fold > di- σ \gg π . The 3-fold hollow mode is slightly more stable by ~ 4.5 kcal/mol than previous reported results [17], due to the lower coverage considered in this work ($\theta = 0.11$ ML vs. $\theta = 0.25$ ML, respectively). The 3-fold and di- σ sites of the regular surface are more stable than those of the stepped surface by 9.7 kcal/mol and 8.8 kcal/mol, respectively. To our knowledge, no experimental or theoretical studies related to the 2-butyne adsorption on metallic surfaces have been published. Our results show that 2-butyne adsorbed on 3-fold hollow sites is the energetically preferred adsorption mode. Although the geometry optimizations were performed without symmetry constraints, the di- σ adsorption mode for 2-butyne was not found. The 3-fold hollow sites on Pd(111) are much more stable than on the stepped surface by 19.3 kcal/mol. The alkyne adsorptions on the stepped surface are disfavoured because these molecules have a high electrophilicity and, at the same time, the Pd atoms belonging to the edge of the step present lower coordination number, with a consequently reduced electron density. We notice that the adsorption geometry for acetylene and 2-butyne is very similar in both considered surfaces. Furthermore, the geometrical parameters for acetylene on the three sites are in agreement with previous theoretical results [17].

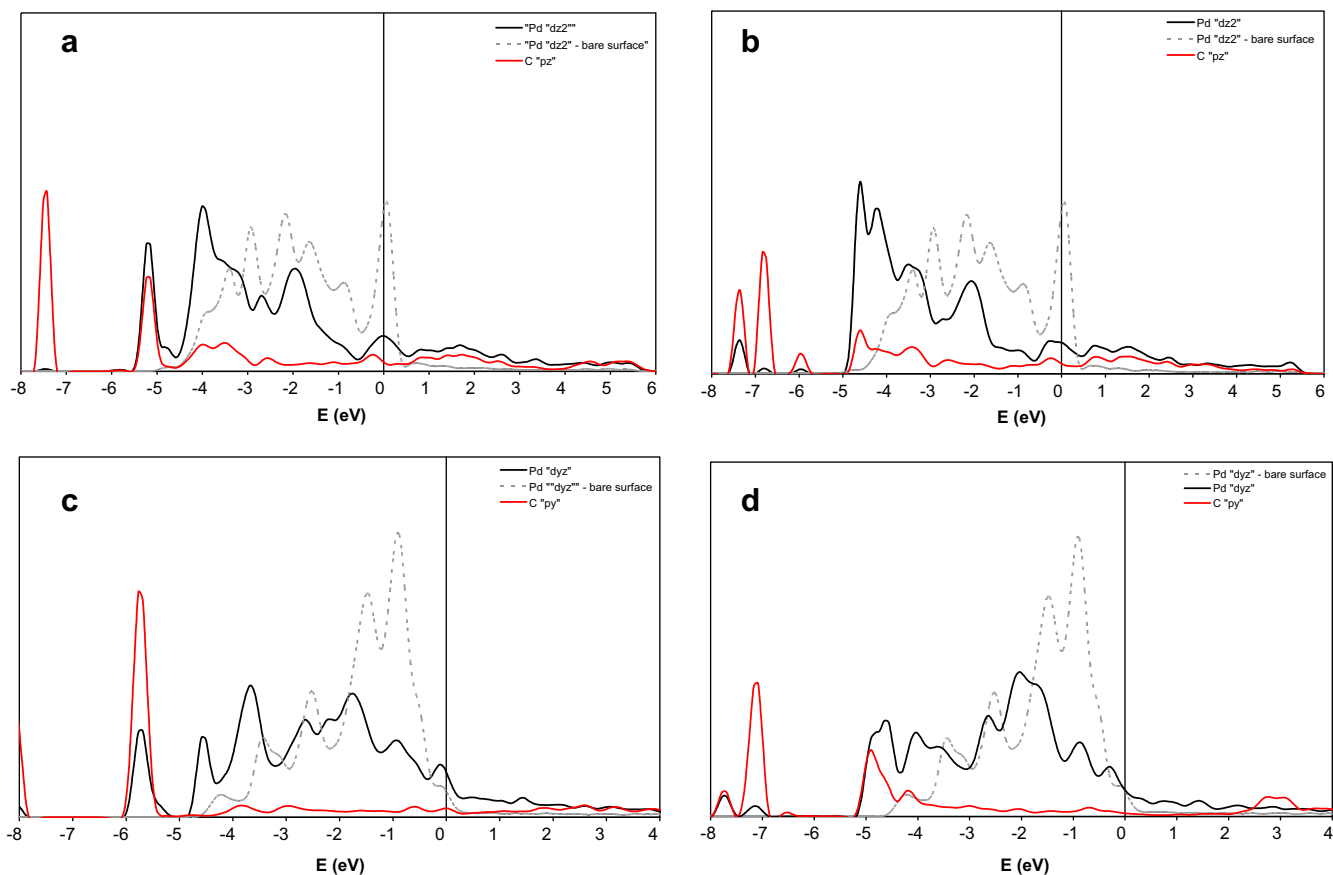


Fig. 5. LDOS for acetylene and 2-butyne molecules adsorbed on the stepped Pd surface. On di- σ site: (a) acetylene and (b) 2-butyne. On 3-fold hollow site: (c) acetylene and (d) 2-butyne.

Table 4

Adsorption energies (E_{ads} in kcal/mol), work function change ($\Delta\Phi$ in eV), dipole moments (μ in Debye) and relevant geometric parameters of alkynes adsorbed on surface Pd(1 1 1).^a

Adsorbate	Acetylene			2-Butyne	
	di- σ	π	3-Fold	π	3-Fold
E_{ads}	-39.9	-19.8	-51.3	-15.3	-43.7
$\Delta\Phi$	-0.96	-1.26	-0.99	-2.21	-1.90
$\Delta\mu$	-1.84	-2.53	-1.94	-4.57	-3.80
$\mu_{\text{adsorbate}}$	-1.51	-0.94	-1.54	-1.51	-2.19
μ_{transf}	-0.30	-1.58	-0.40	-3.06	-1.61
d(Pd-C)	1.99	2.12	2.01	2.13	2.02
d(C \equiv C)	1.32	1.26	1.37	1.27	1.39
d(C-C)	-	-	-	1.47	1.50
C-C \equiv C ^b	131.3	153.6	127.5	149.9	125.9
(Pd-C \equiv C)	112.6	72.6	71.5	72.6	71.5
(Pd-Pd-C)	67.4	76.4	68.7	78.3	69.4

^a Distances expressed in Armstrong (\AA) and bond angles in degrees ($^\circ$).

^b In case of acetylene molecule the angle corresponds to H-C \equiv C.

Looking at the $\Delta\Phi$ values from Table 3, they are greater for Pd(1 1 1) than for the stepped surface, due to the higher coverage of the alkynes in the first surface. Besides, $\Delta\mu$ increases accordingly with the enhancement of $\Delta\Phi$. For both alkynes, the $\mu_{\text{adsorbate}}$ values are similar to those obtained for Pd(4 2 2). This behavior can be explained considering that the internal geometries differences of the alkynes on both surfaces do not alter significantly this parameter. For acetylene, the value of the μ_{transf} is more negative on Pd(1 1 1) in comparison with Pd(4 2 2), indicating that on the former surface the adsorptions are governed by stronger donation effects of the molecules than back-donation effects.

In alkyne hydrogenation, the main objective is to achieve the highest possible alkene selectivity. Several experimental studies devoted to study the particle size effects on the alkyne transformations are rather controversial. Most of these investigations showed that the alkyne hydrogenation is a structure-sensitive reaction at high dispersions, producing specific activity decrement or exhibiting slightly higher activity ([12] and reference therein). In the last years, some new contributions on the alkyne hydrogenation were discovered [47,51,52]. The selective hydrogenation of alkyne to alkene on Pd catalysts was observed when significant amount of sub-surface carbon was present. The effect of carbon dissolution in the crystal lattice near the surface was evidenced by high-resolution transmission electron microscopy [51]. The possible role of this Pd-C phase is to inhibit the emergence of bulk-dissolved hydrogen to the surface, which is reactive but unselective. Besides, the hydrogenation selectivity depends strongly on the H_2 partial pressure; at low pressure the selectivity to alkenes is increased.

The experiments show that, at the initial state of reaction, palladium particles with the proper surface orientation or significant structural defects are required to start the C-C dissociation [51]. Our theoretical results predict a decrease of the binding energy on the stepped Pd(4 2 2) surface of approximately 20% and 44% for acetylene and 2-butyne, respectively, in comparison with the regular Pd(1 1 1) surface. The extremely higher adsorption energies of alkynes on 3-fold hollow sites of bare Pd(1 1 1) imply a very strong bond with the metal surface and, as a consequence, these molecules could be susceptible to decomposition. This fact is confirmed by the geometrical parameters of alkynes adsorbed on this site (lower Pd-C distances and bigger C \equiv C distances than stepped surface). If we consider that in the initial state of reaction the Pd-C phase is not present, our results point out that alkynes would easier dissociate on Pd(1 1 1) than on stepped surfaces or on superficial Pd atoms with low coordination number. Previous DFT calculations showed that the insertion of impurities such as C into the first layer of Pd(1 1 1) surface is energetically favored, being the

C subsurface preferentially trapped in octahedral sites [53]. However, the C diffusion toward the bulk, that is, the C migration from the first to the second surface layers of the solid is an energetically expensive process. From these experimental and theoretical considerations, we can conclude that the alkyne initially decomposes on bare Pd(1 1 1) surface but the carbon diffusion progresses only up to the first interlayer, which is experimentally evidenced by a weak palladium peak with a binding energy of 335.7 eV [51].

A high selectivity in alkyne hydrogenations is possible only if the reactant is easily fragmented at the bare palladium surface and if this surface has ability to build up the superficial Pd-C phase. Different crystal facets will have different activities in the carbon dissolution process. For this reason, further theoretical studies should be performed to evaluate the C diffusion on the stepped surface to arrive toward some conclusion on the role of non-perfect Pd surface in the selective alkyne hydrogenation.

4. Conclusions

In this work, different binding modes and energies for unsaturated hydrocarbons on the stepped Pd(4 2 2) and regular Pd(1 1 1) surfaces were studied. In general, the olefins adsorb preferentially on the stepped surface excepting the 1-butene molecule. On Pd(4 2 2), the adsorption energies for the different butenes change in the order: *trans*-2-butene > *cis*-2-butene \gg 1-butene, with an energy difference of 27% for 1-butene with respect to *trans*-2-butene. Conversely on Pd(1 1 1), the binding energies follow the order: 1-butene > *cis*-2-butene > *trans*-2-butene, with a slightly poor difference between them (nearly 5%). For both surfaces, the electronic charge donation from the olefin molecule is higher than the back-donation from the metal; but the former is relatively higher on π than on di- σ sites, making the adsorption on π sites less stable. Considering the adsorption energy difference between defective and non-defective surfaces, we could infer that the 1-butene hydrogenation occurs on Pd(1 1 1) facets of the Pd catalytic particles instead of the line defects or on Pd atoms with low coordination number.

Regarding the alkynes adsorption, both acetylene and 2-butyne adsorb preferentially on 3-fold sites of the stepped Pd(4 2 2) and regular Pd(1 1 1) surfaces. The binding energies are lower on Pd(4 2 2) than on Pd(1 1 1), with an energy difference of 20% for acetylene and 44% for 2-butyne. In spite of the presence of methyl groups, 2-butyne shows similar internal geometry than acetylene on both surfaces. The higher electrophilicity of alkynes in comparison with olefins generates their stronger adsorptions on electron-rich surfaces like Pd(1 1 1). This behavior could be the reason of their molecular dissociations into C_1 species, beginning the formation of a Pd-C phase as it was experimentally observed in alkyne hydrogenation catalysts.

Acknowledgements

The authors would like to acknowledge the financial support of Universidad Nacional del Sur, CONICET and ANPCyT of Argentina.

References

- [1] G.C. Bond, *Metal-Catalyzed Reactions of Hydrocarbons*, Springer, New York, 2005.
- [2] B. Chen, U. Dingerdissen, J.G.E. Krauter, H.G.J. Lansink Rotgerink, K. Möbus, D.J. Ostgard, P. Panster, T.H. Riermeier, S. Seebald, T. Tacke, H. Trauthwein, *Appl. Catal. A* 280 (2005) 17.
- [3] M.W. Brown, A. Penlidis, G. Sullivan, *Can. J. Chem. Eng.* 69 (1991) 152.
- [4] C.N. Thanh, B. Didillon, P. Sarrazin, C. Cameron, *Selective Hydrogenation Catalyst and a Process Using that Catalyst*. US Patent, 2000.
- [5] Y. Jin, A.K. Datye, E. Rightor, R. Gulotty, W. Waterman, M. Smith, M. Holbrook, J. Maj, J. Blackson, *J. Catal.* 203 (2001) 292.
- [6] A.J. Wright, A.L. Mihele, L.L. Diosady, *Food Res. Int.* 36 (2003) 797.

- [7] A.J. Wright, A. Wong, L.L. Diosady, *Food Res. Int.* 36 (2003) 1069.
- [8] A. Sarkany, Z. Zsoldos, B. Furlong, J.W. Hightower, L. Guzzi, *J. Catal.* 141 (1993) 566.
- [9] A. Sarkany, Z. Zsoldos, Gy. Stefler, J.W. Hightower, L. Guzzi, *J. Catal.* 157 (1995) 179.
- [10] H. Pines, *The Chemistry of Catalytic Hydrocarbon Conversions*, Academic Press, New York, 1981 (Chapter 3).
- [11] Ch. Yoon, M.X. Yang, G.A. Somorjai, *J. Catal.* 176 (1998) 35.
- [12] A. Molnár, *J. Mol. Catal. A* 173 (2001) 185.
- [13] T.G. Rucker, M.A. Logan, T.M. Gentle, E.L. Muetterties, G.A. Somorjai, *J. Phys. Chem.* 90 (1986) 2703.
- [14] W.Y. Kim, H. Hayashi, T.M. Kishida, H. Nagata, K. Wakabayashi, *Appl. Catal. A* 169 (1998) 157.
- [15] M. Neurock, R.A. van Santen, *J. Phys. Chem. B* 104 (2000) 11127.
- [16] J.W. Medlin, M.D. Allendorf, *J. Phys. Chem. B* 107 (2003) 217.
- [17] F. Mittendorfer, C. Thomazeau, P. Raybaud, H. Toulhoat, *J. Phys. Chem. B* 107 (2003) 12287.
- [18] P.A. Sheth, M. Neurock, C.M. Smith, *J. Phys. Chem. B* 107 (2003) 2009.
- [19] A. Valcárcel, A. Clotet, J.M. Ricart, F. Illas, *Chem. Phys.* 309 (2005) 33.
- [20] P.A. Sheth, M. Neurock, C.M. Smith, *J. Phys. Chem. B* 109 (2005) 12449.
- [21] A. Valcárcel, A. Clotet, J.M. Ricart, F. Delbecq, P. Sautet, *J. Phys. Chem. B* 109 (2005) 14175.
- [22] M. Saeys, M.-F. Reyniers, M. Neurock, G.B. Marin, *Surf. Sci.* 600 (2006) 3121.
- [23] L.E. Murillo, A.M. Goda, J.G. Chen, *J. Am. Chem. Soc.* 129 (2007) 7101.
- [24] A.M. Goda, M. Neurock, M.A. Barbeau, J.G. Chen, *Surf. Sci.* 602 (2008) 2523.
- [25] G.C. Bond, *Metal-Catalyzed Reactions of Hydrocarbons, Fundamental and Applied Catalysis Series*, Springer-Verlag, New York, 2005. pp. 395–435.
- [26] G. Kresse, J. Hafner, *Phys. Rev. B* 47 (1993) 558.
- [27] G. Kresse, J. Hafner, *Phys. Rev. B* 48 (1993) 13115.
- [28] G. Kresse, J. Hafner, *Phys. Rev. B* 49 (1994) 14251.
- [29] P. Blochl, *Phys. Rev. B* 50 (1994) 17953.
- [30] G. Kresse, D. Joubert, *Phys. Rev. B* 59 (1999) 1758.
- [31] J.P. Perdew, J.A. Chevary, S.H. Vosko, K.A. Jackson, M.R. Pederson, D.J. Singh, C. Fiolhais, *Phys. Rev. B* 46 (1992) 6671.
- [32] J.P. Perdew, J.A. Chevary, S.H. Vosko, K.A. Jackson, M.R. Pederson, D.J. Singh, C. Fiolhais, *Phys. Rev. B* 48 (1993) 4978.
- [33] H.J. Monkhorst, J.D. Pack, *Phys. Rev. B* 13 (1976) 5188.
- [34] M. Methfessel, A.T. Paxton, *Phys. Rev. B* 40 (1989) 3616.
- [35] F. Raouafi, C. Barreateau, M.C. Desjonquères, D. Spanjaard, *Surf. Sci.* 505 (2002) 183.
- [36] B. Lang, R.W. Joyner, G.A. Somorjai, *Surf. Sci.* 30 (1972) 440.
- [37] M. Mavrikakis, B. Hammer, J.K. Nørskov, *Phys. Rev. Lett.* 81 (1998) 2819.
- [38] M.C. Desjonquères, D. Spaanjard, *Concepts in Surface Physics*, Springer Series in Surface Science, vol. 30, Springer-Verlag, Berlin, 1993.
- [39] A. Valcárcel, A. Clotet, J.M. Ricart, F. Delbecq, P. Sautet, *Surf. Sci.* 549 (2004) 121.
- [40] P.C. Rusu, G. Brocks, *Phys. Rev. B* 74 (2006) 073414.
- [41] J.-S. Filhol, D. Simon, P. Sautet, *J. Phys. Chem. B* 107 (2003) 1604.
- [42] V. Pallassana, M. Neurock, V.S. Lusvardi, J.J. Lerou, D.D. Kragten, R.A. van Santen, *J. Phys. Chem. B* 106 (2002) 1656.
- [43] J. Silvestre-Albero, G. Rupprechter, H.-J. Freund, *J. Catal.* 235 (2005) 52.
- [44] J. Silvestre-Albero, Marta Borasio, G. Rupprechter, H.-J. Freund, *Catal. Commun.* 8 (2007) 292.
- [45] J. Silvestre-Albero, G. Rupprechter, H.-J. Freund, *Chem. Commun.* (2006) 80.
- [46] J. Silvestre-Albero, G. Rupprechter, H.J. Freund, *J. Catal.* 240 (2006) 58.
- [47] D. Teschner, Z. Révay, J. Borsodi, M. Hävecker, A. Knop-Gericke, Robert Schlögl, D. Milroy, S.D. Jackson, D. Torres, P. Sautet, *Angew. Chem.* 120 (2008) 9414.
- [48] H. Hoffmann, F. Zaera, R.M. Ormerod, R.M. Lambert, J.M. Yao, D.K. Saldin, L.P. Wang, D.W. Bennett, W.T. Tysoe, *Surf. Sci.* 268 (1992) 1.
- [49] J.C. Dunphy, M. Rose, S. Behler, D.F. Ogletree, M. Salmeron, *Phys. Rev. B* 57 (1998) R12707.
- [50] H. Sellars, *J. Phys. Chem.* 94 (1990) 8329.
- [51] D. Teschner, E. Vass, M. Hävecker, S. Zafeirotos, P. Schnörch, H. Sauer, A. Knop-Gericke, R. Schlögl, M. Chamam, A. Wootsch, A.S. Canning, J.J. Gammann, S.D. Jackson, J. McGregor, L.F. Gladden, *J. Catal.* 242 (2006) 26.
- [52] D. Teschner, J. Borsodi, A. Wootsch, Z. Révay, M. Hävecker, A. Knop-Gericke, S.D. Jackson, *Science* 86 (2008) 320.
- [53] L. Gracia, M. Calatayud, J. Andrés, C. Minot, M. Salmeron, *Phys. Rev. B* 71 (2005) 033407.